Supplementary Information for

Peptide-lipid nanoparticle-mediated delivery of p53-circRNA synergizes with everolimus for dual suppression of PI3K/AKT/mTOR pathway

Weisi Yuan[1], Qihan Xie[1], Meiping Song[1], Yinan Du[1], Xiaonan Zhang[1], Yan Mu[2], Jiabao Sheng[1], Xing-Jie Liang[2]*, Yinan Zhao[1]* & Shubiao Zhang[1*]

[1]*Key Laboratory of Biotechnology and Bioresources Utilization of the Ministry of Education, Dalian Minzu University; Dalian 116600, P.R. China*

[2]*CAS Center for Excellence in Nanoscience, Chinese Academy of Sciences Key Laboratory for Biological Effects of Nanomaterials and Nanosafety, National Center for Nanoscience and Technology of China, Chinese Academy of Sciences (CAS); Beijing 100190, P.R. China*

[*]Corresponding author: zsb@dlnu.edu.cn; yinanzhao@dlnu.edu.cn; liangxj@nanoctr.cn

Supplementary Figure 1 Schematic diagram illustrating the structural components of synthetic mRNA, including the anti-reverse cap analog (ARCA), 5′ and 3′ untranslated regions (UTR), open reading frame (ORF), and polyadenylate (Poly-A) tail.

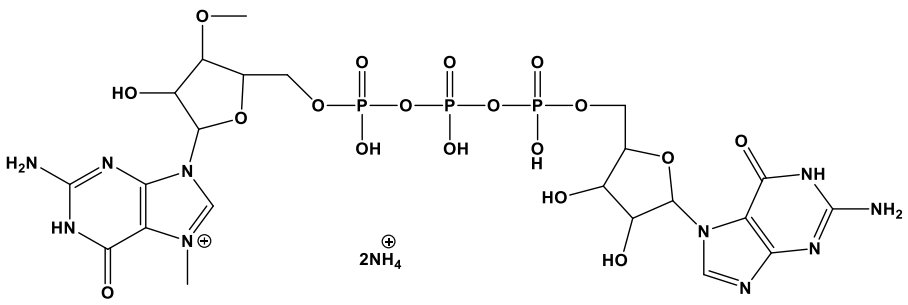

Supplementary Figure 2 The molecular structure of 5′ cap analog 3′-O-methyl-m7GpppG-ARCA, showing the methyl modifications at N7 position of guanosine and 3′-O position.

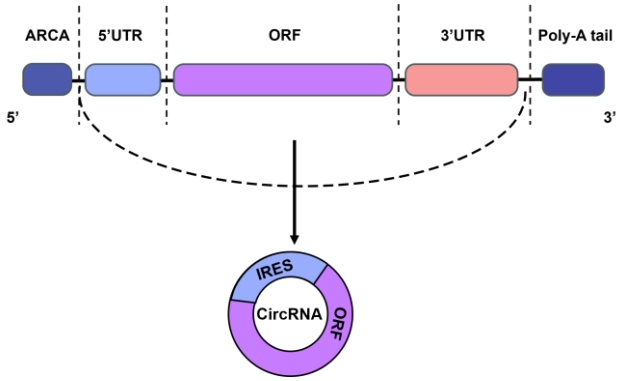

Supplementary Figure 3 Structure of CircRNA. Through pre-mRNA backsplicing, the linear transcript is circularized to form p53-CircRNA. This circular RNA molecule adopts a covalently closed structure and lacks both a 5′ cap and a 3′ poly(A) tail.

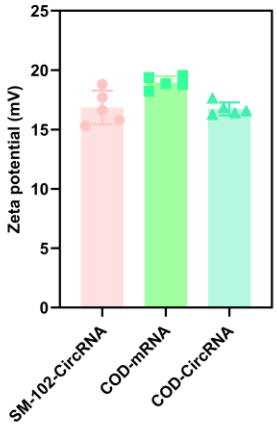

Supplementary Figure 4 Zeta potential of the LNPs. Data were shown as mean ± SEM (n = 5).

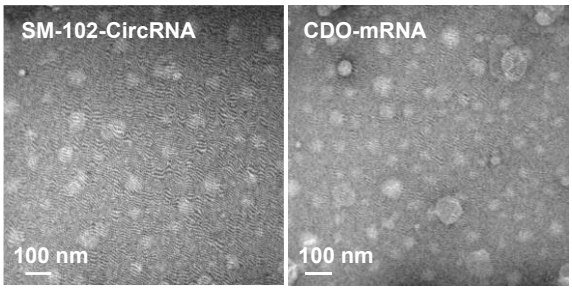

Supplementary Figure 5 Representative TEM images of SM-102-CircRNA and CDO-mRNA LNPs.

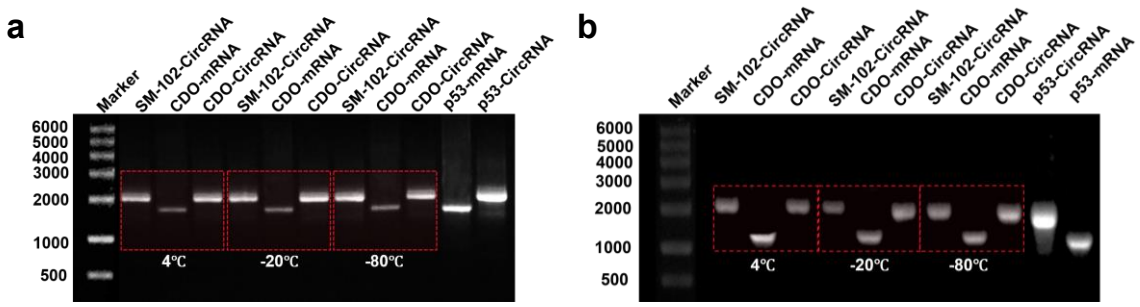

Supplementary Figure 6 Electrophoretic analysis of RNA degradation in LNPs following storage at 4 °C, -20 °C, and -80 °C for (**a**) 1 month and (**b**) 2 months.

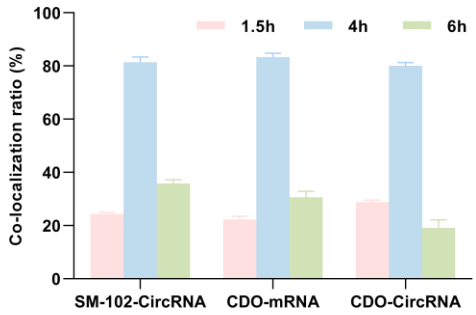

Supplementary Figure 7 Quantification of the co-localization between Cy5-labeled RNA (red) and lysosomes (green) from 5-6 randomly selected cells per group.

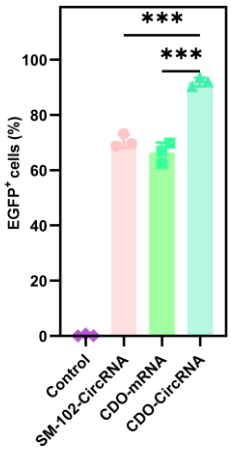

Supplementary Figure 8 *In vitro* transfection efficiency, presented as the percentage of EGFP-positive cells, was analyzed by flow cytometry. Data were shown as mean ± SEM (n = 3). Statistical significance was determined by a two-tailed t-test (*** $p < 0.001$).

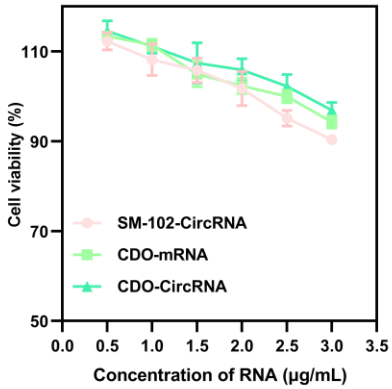

Supplementary Figure 9 Viability of normal human bronchial epithelial cells (BEAS-2B) treated with CDO-CircRNA, CDO-mRNA, or SM-102-CircRNA, as determined by CCK-8 assay. Cells were exposed to increasing concentrations (0.5 to 3.0 μg/mL) of each RNA to assess dose-dependent effects on cell viability. Data were presented as mean ± SEM (n = 3).

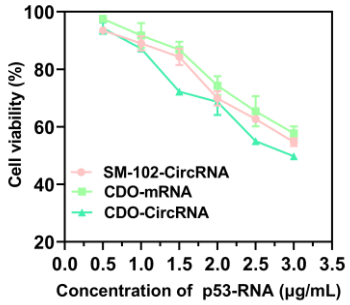

Supplementary Figure 10 Viability of human non-small cell lung carcinoma cells (NCI-H1299) following treatment with CDO-CircRNA, CDO-mRNA, or SM-102-CircRNA. Cell viability was determined by CCK-8 assay after exposure to the indicated RNAs at a concentration range of 0.5 to 3.0 μg/mL. Data were presented as mean ± SEM (n = 3).

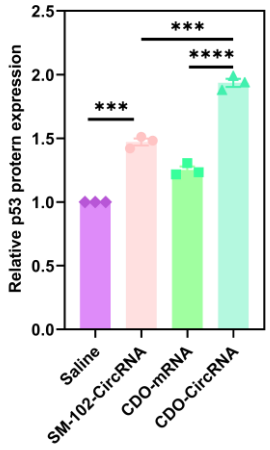

Supplementary Figure 11 Relative p53 protein expression levels. Data were represented as mean ± SEM ($n = 3$). Statistical significance was determined by a two-tailed *t*-test (*** $p < 0.001$; **** $p < 0.0001$).

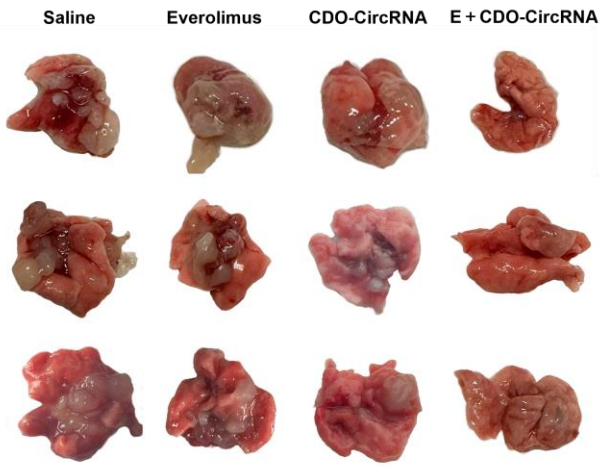

Supplementary Figure 12 Lung morphology images from orthotopic tumor-bearing mice following treatment administration.

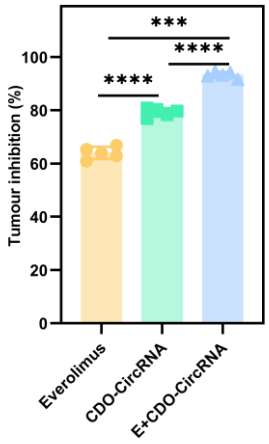

Supplementary Figure 13 Tumor growth inhibition in orthotopic tumor-bearing mice following 21 days of treatment**.** Data were represented as mean ± SEM (n = 5). Statistical significance was determined by a two-tailed t-test (*** $p < 0.001$; **** $p < 0.0001$).

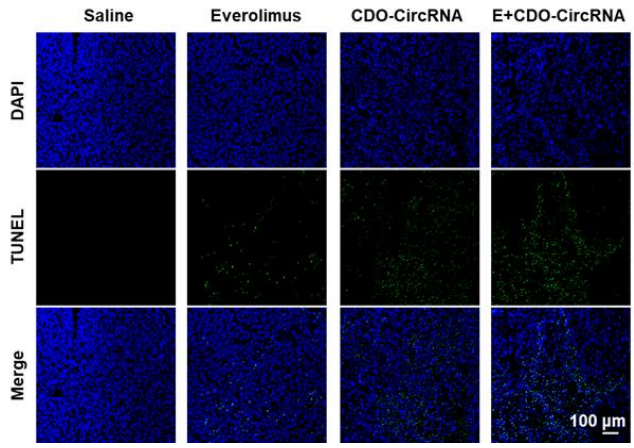

Supplementary Figure 14 Apoptosis in tumor cells from orthotopic tumor-bearing mice was assessed by TUNEL assay. Nuclei were counterstained with DAPI (blue), and apoptotic cells were labeled in green. Scale bar: 100 μm.

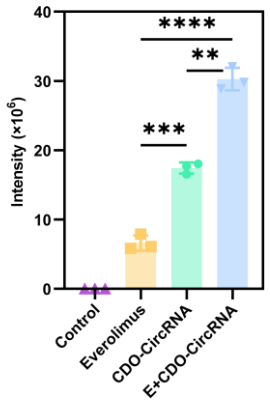

Supplementary Figure 15 Quantitative analysis of apoptosis in tumor cells from orthotopic tumor-bearing mice, measured by integrated fluorescence intensity of TUNEL staining. Data were presented as mean ± SEM (n = 3). Statistical significance was determined using two-tailed t-test (** $p < 0.01$; *** $p < 0.001$; **** $p < 0.0001$).

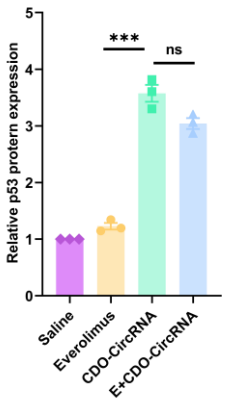

Supplementary Figure 16 Relative p53 protein expression levels in lung tumor tissues from orthotopic tumor-bearing mice following treatment with everolimus, CDO-CircRNA, or their combination (E+CDO-CircRNA). Data were shown as mean ± SEM (*n* = 3).

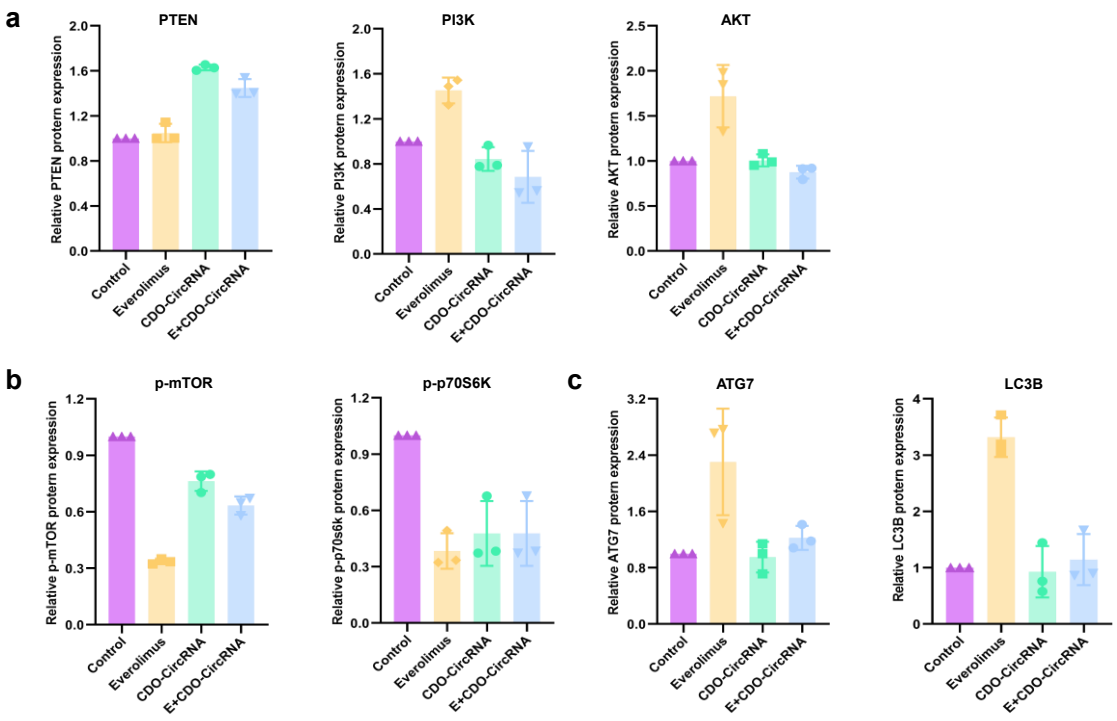

Supplementary Figure 17 Analysis of key protein expression in NSCLC orthotopic tumors by Western blot. **a** Relative expression levels of PTEN, PI3K, and AKT, key components of the PI3K/AKT pathway. **b** Phosphorylation levels of mTOR and its downstream target p70S6K. **c** Expression of the autophagy-related proteins ATG7 and LC3B-II. Data were shown as mean ± SEM (n = 3).

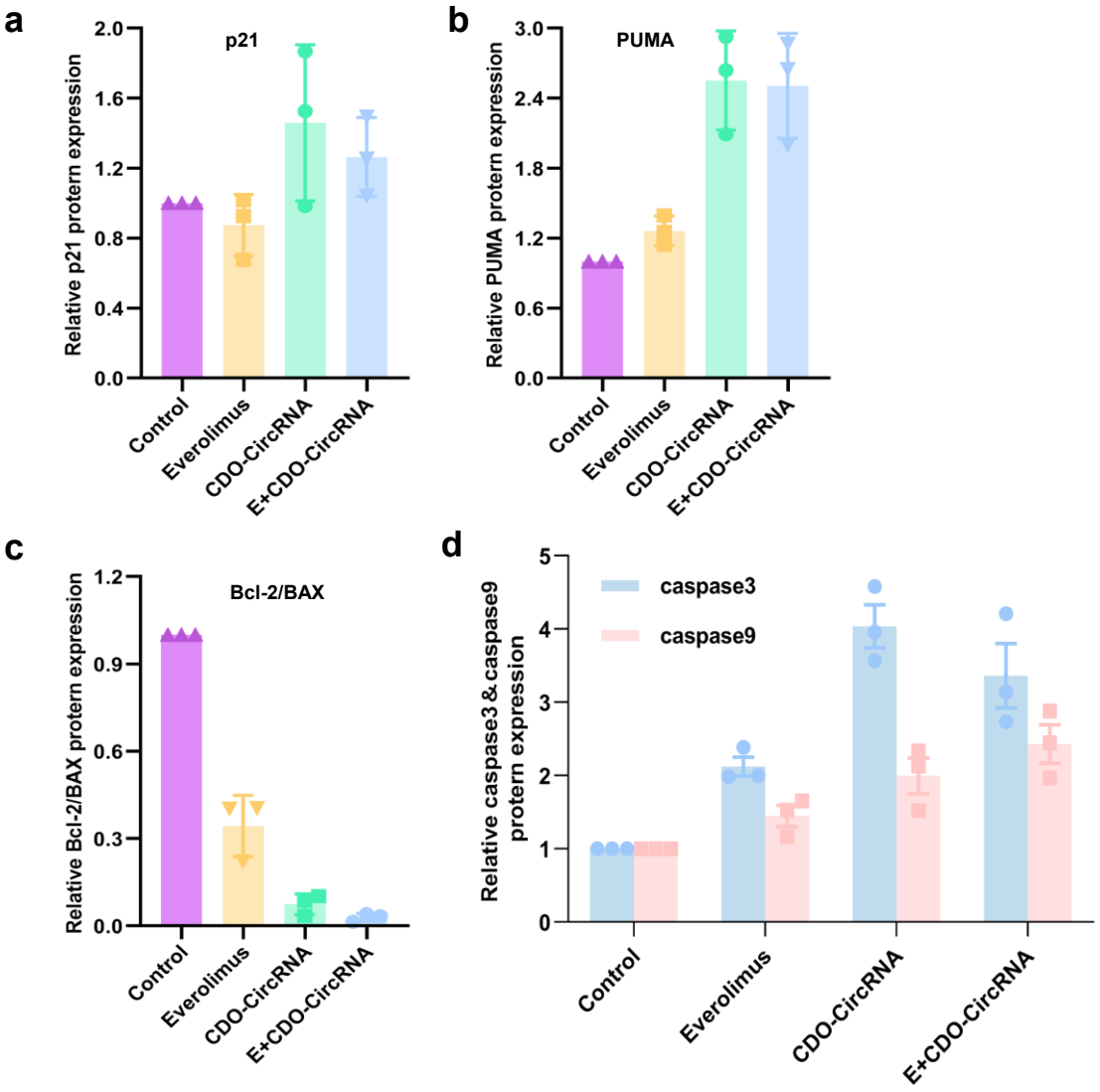

Supplementary Figure 18 Quantitative Western blot analysis of apoptosis-related proteins in orthotopic NSCLC tumor tissues. **a** Expression of the cell cycle regulator p21. **b** Expression of the p53 upstream regulator PUMA. **c** The calculated Bcl-2/Bax ratio. **d** Expression levels of the key apoptosis executers, Cleaved Caspase-9 and Cleaved Caspase-3. Data were shown as mean ± SEM (n = 3).

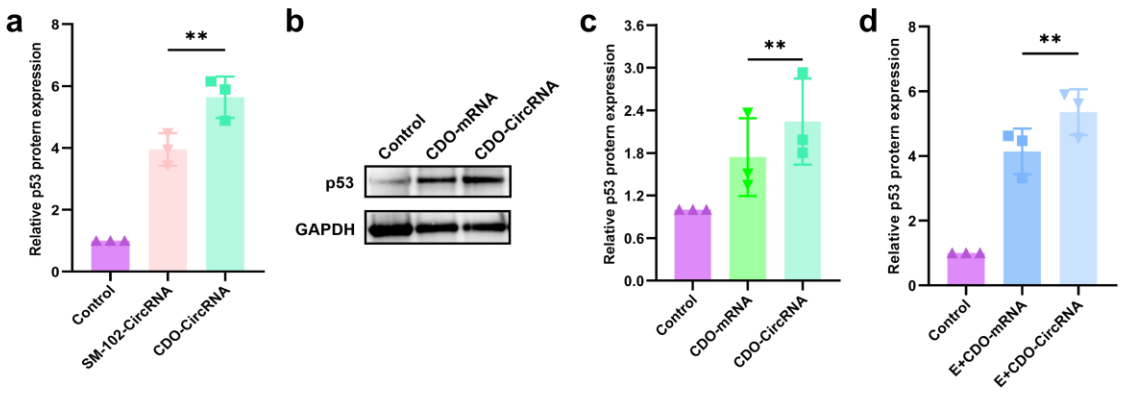

Supplementary Figure 19 Analysis of p53 protein expression in orthotopic NSCLC tumors mediated by different LNPs and RNA forms. **a** p53 expression following treatment with CDO-CircRNA compared with SM-102-CircRNA. **b** p53 expression in tumors treated with E+CDO-CircRNA versus E+CDO-mRNA, assessed by Western blotting. **c** p53 expression mediated by CDO-CircRNA relative to CDO-mRNA. **d** p53 expression levels in the E+CDO-CircRNA group compared to the E+CDO-mRNA group. Data were presented as mean ± SEM (n = 3). Statistical significance was determined using two-tailed t-test (** $p < 0.01$.).

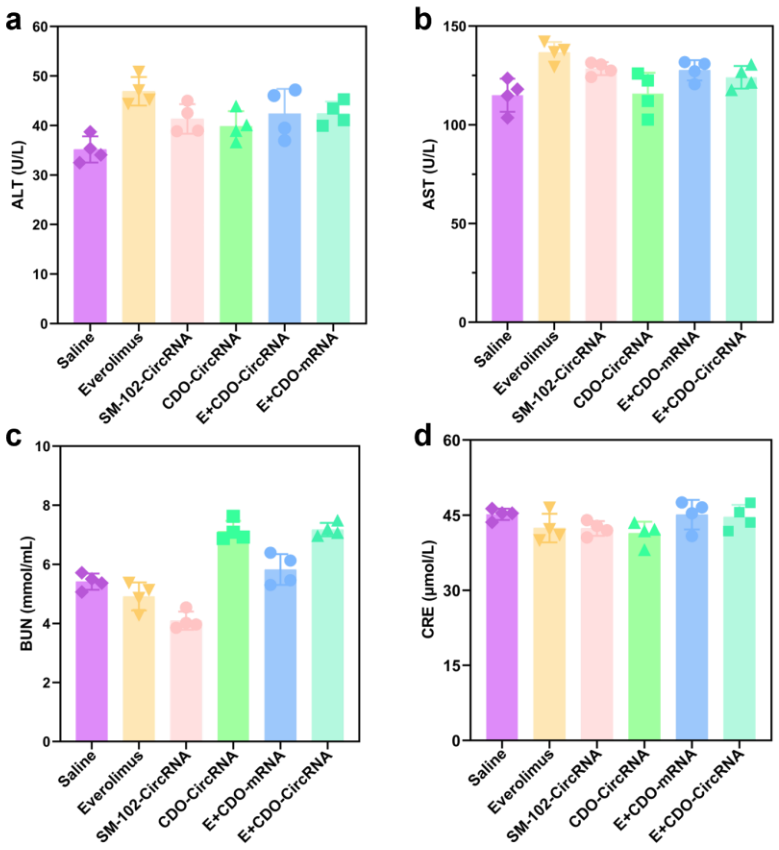

Supplementary Figure 20 Toxicity evaluation of LNPs through hepatic and renal function analysis. **a** Alanine aminotransferase (ALT) activity. **b** Aspartate aminotransferase (AST) activity. **c** Blood urea nitrogen (BUN) levels. **d** Creatinine (CRE) concentration. Data represent mean ± SD from five animals per group. Data were shown as mean ± SEM (n = 4).

Supplementary Table 1 Lipid composition of different LNPs.

Sample Name	N/P (wt/wt)	RNA Forms	Lipid Compositions
SM-102-CircRNA	20:1	CircRNA	SM-102：DOPE：CHOL：DSPE-PEG2000
CDO-mRNA	20:1	mRNA	CDO：DOPE：CHOL：DSPE-PEG2000
CDO-CircRNA	20:1	CircRNA	CDO：DOPE：CHOL：DSPE-PEG2000

Supplementary Table 2 Different *p53*-RNA sequences used in this study.

Type of *p53*-RNA	Sequence
Human *p53*-RNA Open Reading Frame (ORF) sequence：	AUGGAGGAGCCGCAGUCAGAUCCUAGCGUCGAGCCC CCUCUGAGUCAGGAAACAUUUUCAGACCUAUGGAAAC UACUUCCUGAAAACAACGUUCUGUCCCCCUUGCCGU CCCAAGCAAUGGAUGAUUUGAUGCUGUCCCCGGACG AUAUUGAACAAUGGUUCACUGAAGACCCAGGUCCAGA UGAAGCUCCCAGAAUGCCAGAGGCUGCUCCCCCCGU GGCCCCUGCACCAGCAGCUCCUACACCGGCGGCCCC UGCACCAGCCCCCUCCUGGCCCCUGUCAUCUUCUGU CCCUUCCCAGAAAACCUACCAGGGCAGCUACGGUUU CCGUCUGGGCUUCUUGCAUUCUGGGACAGCCAAGUC UGUGACUUGCACGUACUCCCCUGCCCUCAACAAGAU GUUUUGCCAACUGGCCAAGACCUGCCCUGUGCAGCU GUGGGUUGAUUCCACACCCCCGCCCGGCACCCGCGU CCGCGCCAUGGCCAUCUACAAGCAGUCACAGCACAU GACGGAGGUUGUGAGGCGCUGCCCCCACCAUGAGCG CUGCUCAGAUAGCGAUGGUCUGGCCCCUCCUCAGCA UCUUAUCCGAGUGGAAGGAAAUUUGCGUGUGGAGUA UUUGGAUGACAGAAACACUUUUCGACAUAGUGUGGU GGUGCCCUAUGAGCCGCCUGAGGUUGGCUCUGACU GUACCACCAUCCACUACAACUACAUGUGUAACAGUUC CUGCAUGGGCGGCAUGAACCGGAGGCCCAUCCUCAC CAUCAUCACACUGGAAGACUCCAGUGGUAAUCUACU GGGACGGAACAGCUUUGAGGUGCGUGUUUGUGCCU GUCCUGGGAGAGACCGGCGCACAGAGGAAGAGAAUC UCCGCAAGAAAGGGGAGCCUCACCACGAGCUGCCCC CAGGGAGCACUAAGCGAGCACUGCCCAACAACACCA GCUCCUCUCCCCAGCCAAAGAAGAAACCACUGGAUG GAGAAUAUUUCACCCUUCAGAUCCGUGGGCGUGAGC GCUUCGAGAUGUUCCGAGAGCUGAAUGAGGCCUUGG AACUCAAGGAUGCCCAGGCUGGGAAGGAGCCAGGGG GGAGCAGGGCUCACUCCAGCCACCUGAAGUCCAAAA AGGGUCAGUCUACCUCCCGCCAUAAAAAACUCAUGUU CAAGACAGAAGGGCCUGACUCAGACUGA